Mechanical Properties of Teak Wood Flour-Reinforced HDPE Composites

Kamini Sewda, S. N. Maiti

Centre for Polymer Science and Engineering, Indian Institute of Technology Delhi, New Delhi 110016, India

Received 3 April 2008; accepted 17 November 2008
DOI 10.1002/app.29696
Published online 11 February 2009 in Wiley InterScience (www.interscience.wiley.com).

ABSTRACT: Mechanical properties such as tensile and impact strength behavior of teak wood flour (TWF)-filled high-density polyethylene (HDPE) composites were evaluated at 0–0.32 volume fraction (Φ_f) of TWF. Tensile modulus and strength initially increased up to $\Phi_f = 0.09$, whereas a decrease is observed with further increase in the Φ_f. Elongation-at-break and Izod impact strength decreased significantly with increase in the Φ_f. The crystallinity of HDPE also decreased with increase in the TWF concentration. The initial increase in the tensile modulus and strength was attributed to the mechanical restraint, whereas decrease in the tensile properties at $\Phi_f > 0.09$ was due to the predominant effect of decrease in the crystallinity of HDPE. The mechanical restraint decreased the elongation and Izod impact strength. In the presence of coupling agent, maleic anhydride-grafted HDPE (HDPE-*g*-MAH), the tensile modulus and strength enhanced significantly because of enhanced interphase adhesion. However, the elongation and Izod impact strength decreased because of enhanced mechanical restraint on account of increased phase interactions. Scanning electron microscopy showed a degree of better dispersion of TWF particles because of enhanced phase adhesion in the presence of HDPE-*g*-MAH. © 2009 Wiley Periodicals, Inc. J Appl Polym Sci 112: 1826–1834, 2009

Key words: mechanical properties; high-density polyethylene; teak wood flour; composites; coupling agent; crystallinity; phase adhesion

INTRODUCTION

Wood plastic composites (WPCs) have attracted significant attention worldwide because of ecological and environmental concerns.[1–3] The wood component comprises of wood flour, bark flour, paper pulp, bamboo fiber, wood fiber, and the like.[4–10] Wood-based fillers are incorporated into polymer matrices to achieve decreased manufacturing cost, moderately improved stiffness, light weight, abrasion and creep resistance, and reduced shrinkage. The composites are environmental friendly because of their less dependence on nonrenewable energy/material resources, decreased pollutant and greenhouse gas emissions, enhanced energy recovery, and end-of-life biodegradability.[10–12] WPCs were extensively used in the automotive industries and building applications as flooring material, furniture, interior finishing materials including window frames, bathroom doors, outdoor applications such as garden fencing and decking.[5]

The thermoplastics used for WPCs include high-density polyethylene (HDPE), low-density polyethylene (LDPE), polypropylene (PP), polyvinylchloride (PVC), and polystyrene (PS).[4,10,13–15] A commodity polyolefin, HDPE, has been extensively used because of its excellent chemical and environmental resistance, outstanding electrical insulation, and easy moldability. It can be processed at relatively low temperatures, which was the first requirement for WPCs because wood components start degrading at high temperatures, which makes HDPE as the best candidate for WPCs.[10,16]

The major components of wood flour are cellulose, lignin, and hemicellulose, which contain polar hydroxyl (—OH) groups.[10,17] HDPE is nonpolar as it comprises only aliphatic chains. Thus, WPCs encountered the most important problem of incompatibility between hydrophilic (polar) wood flour and hydrophobic (nonpolar) polymer matrix. This incompatibility results from poor interfacial interaction leading to poor dispersion of the wood flour in HDPE and sequential poor stress transfer between the phases. Coupling agents have played a very important role in enhancing the compatibility and bonding strength between wood flour and nonpolar thermoplastics in WPCs. To improve the interaction between HDPE and wood flour, the use of maleic anhydride-grafted HDPE (HDPE-*g*-MAH) as coupling agent has been reported.[4,5,10,11,18] Being

Correspondence to: S. N. Maiti (maiti@polymers.iitd.ernet.in or maitisn49@yahoo.co.in).

Contract grant sponsor: Council of Scientific and Industrial Research (CSIR) (Research Grant, Senior Research Fellowship).

hygroscopic WPC absorbs moisture, which can also be restricted by the coupling agent.[19–22]

The objectives of this study were to investigate the effects of incorporation of teak wood flour (TWF) (*Tectona grandis*, common name teak wood) on the morphology and mechanical properties of HDPE. The effects of a coupling agent used to modify the surface of the wood flour in the resulting composite properties were examined. Tensile properties were compared with theoretical models to evaluate phase interactions. Impact strength and crystallinity were determined with respect to the filler concentrations. Scanning electron microscopy (SEM) was carried out to characterize the morphology of the composites.

EXPERIMENTAL

Materials

G-Lex I58A180 (Gas Authority of India, GAIL) injection molding grade HDPE ($\rho = 0.95$ g/cc, MFI 18 g/10 min at 230°C and 2160 g load) was used as the matrix.[23] The TWF from sawdust was sieved and the particles of mesh size below 180 μm were used as the filler. The coupling agent used was OPTIM TP-506/E (Pluss Polymers Pvt., India), which is HDPE-*g*-MAH ($\rho = 0.954$ g/cc, MFI = 1.24 g/10 min at 230°C and 2160 g load, maleic anhydride content (%) 0.99, acid number 11).[24] The coupling agent content was 5 wt % on the basis of the filler quantity.

The volume fraction (Φ_f) of TWF in the composites has been calculated following eq. (1):

$$\Phi_f = (W_{\mathrm{TWF}}/\rho_{\mathrm{TWF}})/[(W_{\mathrm{TWF}}/\rho_{\mathrm{TWF}}) + (W_{\mathrm{HDPE}}/\rho_{\mathrm{HDPE}})] \quad (1)$$

where W and ρ denote the mass and density of the components. The density of TWF was determined by the use of specific gravity bottle using vacuum-dried TWF. The value was 1.0018 g cm^{-3}.

Compounding and molding

HDPE was dry blended with the vacuum-dried TWF.[17] Composites of HDPE and TWF were prepared with Φ_f of filler varying from 0 to 0.32 by tumble blending followed by melt compounding in a corotating twin-screw extruder, Model JSW J75E IV-P ($L/D = 36$, $D = 30$ mm), at a screw speed of 174 rpm. The temperatures from the feed zone to the die zone were 140–180°C.[3,25] The extruded strands were quenched in a water bath and then pelletized. The pellets were air-dried for 3 h at 60°C followed by vacuum drying at 65°C for 4 h. The test specimen used for tensile and Izod impact tests were injection-molded on an L and T-Demag injection molding machine (model PFY 40-LNC 4P). The temperatures were 150–180°C from the feed zone to the nozzle maintaining the mold temperature at 30°C. HDPE was extruded and molded under the same processing conditions to maintain similar thermal and shear history to that of the composites.

Tests and measurements

Tensile and impact tests have been conducted in accordance with the ASTM D638, ASTM D256 test methods, respectively.[26] Tensile properties were measured on a Zwick Universal Tester, model Z010, at a cross-head speed 100 mm/min and cross-head separation 60 mm. The notched Izod impact measurements were carried out on a falling hammer type Atsfaar Charpy Impact tester, model Impacts-15. Average value of six samples was reported for each composite composition. All measurements were carried out at an ambient temperature, 30°C ± 2°C.

The crystallinity studies were carried out by the following two methods:

i. The wide angle X-ray diffraction (WAXD) scans were taken in the angular range of $2\theta = 10$–35°, recorded on Philips X-ray diffraction machine (PANalytical diffractometer). The degree of crystallinity was calculated from the X-ray diffraction data as the ratio of the scattering from the crystalline regions, A_{cr}, to the total sample scattering, $A_{\mathrm{am}} + A_{\mathrm{cr}}$, where A_{am} represents the amorphous scattering, eq. (2), (using simple peak area method)[27]:

$$\text{Degree of crystallinity}, X_c(\%) = [A_{\mathrm{cr}}/(A_{\mathrm{cr}} + A_{\mathrm{am}})] \times 100 \quad (2)$$

ii. Differential scanning calorimetery (DSC) was performed on a Perkin–Elmer Pyris-7 calorimeter calibrated with indium. Samples were prepared by filling from three different parts of injection-molded tensile samples. Filled samples were dried for an hour before DSC studies at 60°C and then scanned at the rate of 10°C/min in the temperature ranging from 30 to 150°C, and held for 5 min at 150°C to eliminate the effect of previous thermal history. The samples were then cooled to 30°C at a rate of 10°C/min, again heated to 150°C at 10°C/min and the scan recorded. The degree of crystallinity (%) of HDPE in the composites was evaluated from heat of fusion (ΔH) for each composite composition following eq. (3) and normalized for 5 mg of sample by considering the enthalpy for 100% crystalline polyethylene, ($\Delta H_{\mathrm{theoretical}} = 277$ J/g)[28]:

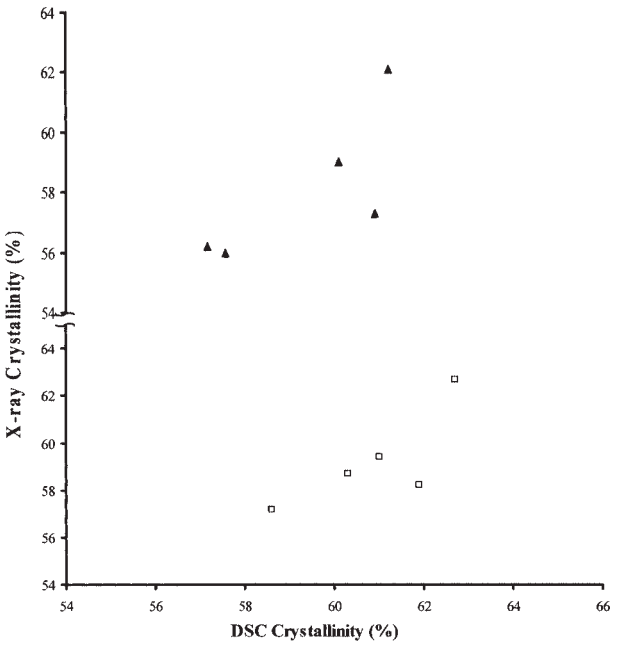

Figure 1 Correlation of crystallinity (%) evaluated from X-ray and DSC methods for HDPE/TWF (□) and HDPE/TWF/HDPE-*g*-MAH (▲) composites.

$$\text{Degree of crystallinity} = [(\Delta H_{\text{experimental}}/W_{\text{HDPE}})/\Delta H_{\text{theoretical}}] \times 100 \quad (3)$$

where W_{HDPE} is weight fraction of HDPE in the composites.

Morphological analysis was carried out by SEM on cryogenically fractured surfaces of the bar samples. All samples were sputtered with silver prior to microscopic studies on a Stereoscan 360.

RESULTS AND DISCUSSION

Crystallinity

HDPE is a semicrystalline polymer and the relative extent of crystalline content of HDPE strongly influences the mechanical properties. The crystallinity data obtained from WAXD method and DSC measurements for HDPE/TWF and HDPE/TWF/HDPE-*g*-MAH systems are in good agreement, Figure 1. This indicates that the crystallinity values evaluated by both the methods are comparable.

Incorporation of TWF filler decreased the crystallinity of HDPE and the decrease continued with increase in Φ_f, which is shown as the plot of normalized crystallinity (X_c) values, i.e., ratio of the crystallinity of HDPE in the composites (subscript *c*) to that of the HDPE (subscript *p*) versus Φ_f for HDPE/TWF and HDPE/TWF/HDPE-*g*-MAH systems, Figure 2. In the HDPE/TWF composites, the decrease in the crystallinity of HDPE is attributed to the mechanical restraints imposed by the TWF particles, which obstruct the HDPE molecules to crystallize properly. In the HDPE/TWF/HDPE-*g*-MAH composites, the chain entanglements between HDPE and HDPE-*g*-MAH along with the chemical interaction of TWF with HDPE-*g*-MAH play additional role in restricting the crystallinity of the HDPE molecules. Thus, the crystallinity of the major phase HDPE will be included in describing the mechanical properties of the composites. In these analyses, the crystallinity (%) of HDPE evaluated by WAXD method (X_c) was used.

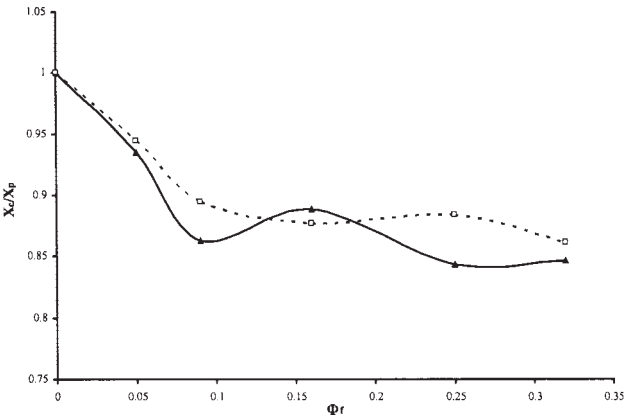

Figure 2 Variation of normalized relative crystallinity evaluated by X-ray method for HDPE/TWF (□----) and HDPE/TWF/HDPE-*g*-MAH (▲——) composites vs. Φ_f.

Tensile properties

The stress–strain curves of the HDPE/TWF composites are plotted in Figure 3 as a function of Φ_f. The stress–strain curve of neat HDPE shows an initial linear increase resulting in a peak (yield peak) and after that stress decreases with increasing strain.

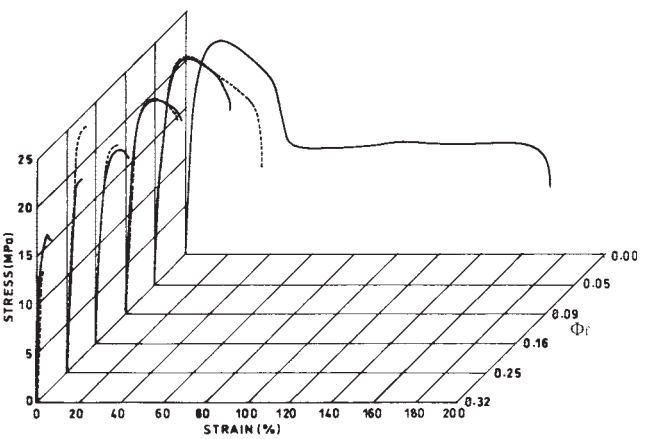

Figure 3 Stress–strain curves of HDPE/TWF (——) and HDPE/TWF/HDPE-*g*-MAH (----) composites as a function of Φ_f.

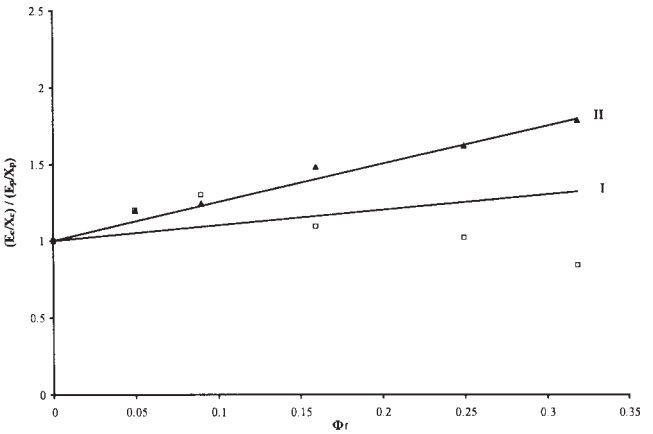

Figure 4 Comparison of normalized relative modulus data of HDPE/TWF (□) and HDPE/TWF/HDPE-*g*-MAH (▲) composites with Einstein model without adhesion, eq. (4), Curve I and Einstein model with adhesion, eq. (5), Curve II, against Φ_f.

Necking starts after the yield peak which ultimately results into the breakage of the sample. HDPE thus shows a ductile failure. For composites, there was a gradual shortening of the curve, the curve ends just beyond the yield point. With increase in Φ_f the curve ends at the yield region. This indicates stiffening of HDPE with accompanied decrease in the toughness as the Φ_f increases.

In the presence of the coupling agent, the general shapes of the curves were similar, Figure 3. The break points were higher in comparison to the corresponding composites without the coupling agent.

Tensile properties, e.g., tensile modulus, breaking strength, and elongation-at-break of the HDPE/TWF composites were evaluated from the stress–strain curves, Figure 3. The ratios of the properties of the composites (subscript *c*) to that of HDPE matrix polymer (subscript *p*) are presented as functions of Φ_f in the subsequent sections.

Tensile modulus

Figure 4 presents the normalized relative tensile moduli (ratio of the normalized moduli of the composites to that of the matrix), $(E_c/X_c)/(E_p/X_p)$, versus Φ_f of the composites. The modulus enhanced to ~ 1.3 at $\Phi_f = 0.09$, the value then decreased to 1–0.7, depending on the Φ_f. The data were compared with predictive models for two phase compositions, where the shapes of the dispersed phase and its packing fraction as well as the phase interactions are taken into account (Fig. 4). Curve I denotes Einstein equation without adhesion,[29–33] [eq. (4)], whereas curve II describes Einstein equation with adhesion, [eq. (5)][29–33]:

$$(E_c/X_c)/(E_p/X_p) = 1 + \Phi_f \quad (4)$$

$$(E_c/X_c)/(E_p/X_p) = 1 + 2.5\Phi_f \quad (5)$$

The data for HDPE/TWF composites were higher than eq. (4) up to $\Phi_f = 0.09$, while the model was higher in the range of $\Phi_f = 0.16$–0.32. Because the moduli values up to $\Phi_f = 0.09$ are higher than unity and the data are normalized which eliminate the variation of crystallinity of HDPE by the TWF, a degree of phase adhesion may be implied. As has been stated in a previous work, the mechanical properties of the composites are functions of phase interactions and their sequential effect on the matrix crystallinity.[6] The TWF contains hydroxyl and carboxylic groups so that chemical interaction with nonpolar HDPE may not be possible. However, physical interaction through mechanical locking of phases may arise because of differential thermal shrinkage of the phases.[31] The wood flour particles do not expand thermally much, whereas that for the fluid HDPE is very high. Upon cooling, the expanded HDPE shrinks more and thus anchors around the TWF particles. During tensile tests, some force will be expended to overcome these anchoring or physical forces, which enhances the modulus value. The TWF may thus give rise to mechanical restraint causing impediment on the deformability of the polymer. The mechanical restraint is a function of TWF particulate spacing as well as the properties of the TWF and the matrix.[34] HDPE is also an olefin polymer whose mechanical properties are thoroughly dependent on its crystallinity. The composite properties will be dependent on the resultant of these opposing factors.

In the HDPE/TWF composites up to $\Phi_f = 0.09$ as the effect of crystallinity in the presence of TWF has been accounted for by normalizing the data, the experimental results directly indicate phase adhesion, in this case, by physical means as stated earlier. However, at $\Phi_f = 0.16$–0.32, the modulus decreased which may be due to the filler agglomeration. The interparticle bonding forces in the agglomerates being very low, the composites fail easily in the absence of phase interactions.

In the presence of the coupling agent, HDPE-*g*-MAH, the normalized relative moduli increase with Φ_f, Figure 4. The data agree well with Einstein equation with adhesion, eq. (5), Figure 4, which implies a good degree of phase adhesion. This adhesion may be attributed to chemical reactions between the hydroxyl and acidic groups of the TWF and anhydride/carboxylic moieties of the HDPE-*g*-MAH as shown in Scheme 1.[20] Similar chemical interactions have been reported in other HDPE/wood cellulose composites also.[6,10,20,35,36] It may be stated that although a low quantity of the coupling agent (5 wt %

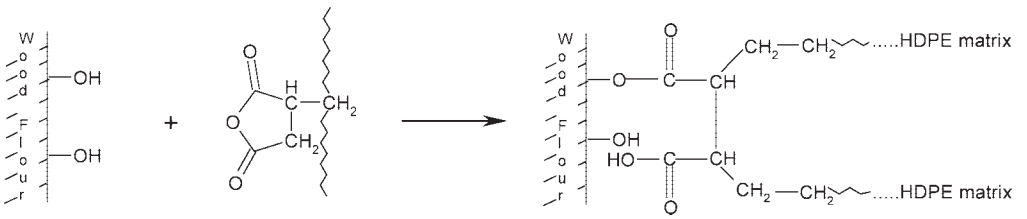

Scheme 1 Interaction between HDPE and wood fluor through HDPE-*g*-MAH.

based on the concentration of TWF) has been employed, the extent of phase interactions is quite significant, so that the modulus is enhanced despite a decrease in the crystallinity of HDPE. The phase adhesions here are due to a combination of both physical and chemical interactions. Increase in modulus was reported in other wood flour/HDPE composites also.[15]

Elongation-at-break

The normalized relative elongation-at-break, $(\varepsilon_c/X_c)/(\varepsilon_p/X_p)$, of HDPE/TWF composites declines drastically with increase in Φ_f, Figure 5. The decrease in elongation was quite drastic at $\Phi_f = 0.05$, the data decrease beyond this Φ_f was marginal, similar to other particulate-filled polymer composites.[6,15] At the highest Φ_f, the value was 0.08 times that of HDPE. With the addition of the coupling agent, HDPE-*g*-MAH, the elongation follows similar decreasing trend at and beyond $\Phi_f = 0.05$. The experimental data were compared with Nielsen's model with perfect adhesion, eq. (6)[31,33]:

$$(\varepsilon_c/X_c)/(\varepsilon_p/X_p) = 1 + \Phi_f^{1/3} \quad (6)$$

where ε_c and ε_p depict the elongation-at-break for the composite and the matrix, respectively. The elongation data were far below the theoretical model. This may be due to the formation of weak composites on account of vacuole formation around the TWF particles in the absence of adhesive bond between the phases. The incorporation of TWF provides mechanical restraints resulting in the discontinuity of matrix, which in turn inhibits the ductility causing decrease in the elongation-at-break. In the presence of the coupling agent, the elongation decrease was lower up to $\Phi_f = 0.09$; however, the data were marginally lower to those with HDPE/TWF systems. This indicates a degree of enhanced adhesion, which led to increased mechanical restraint through chemical interaction between the TWF and the HDPE brought about by the coupling agent. Similar results were reported in other works also.[8,13]

Tensile strength

Figure 6 presents the normalized relative tensile strength (ratio of the normalized tensile strength of the composites to that of the matrix), $(\sigma_c/X_c)/(\sigma_p/X_p)$, versus Φ_f of the composites. In the HDPE/TWF composites, the tensile strength increased up to $\Phi_f = 0.09$, the values then decreased with further increase in Φ_f, the data varying from 1 to 0.9 as Φ_f varied from

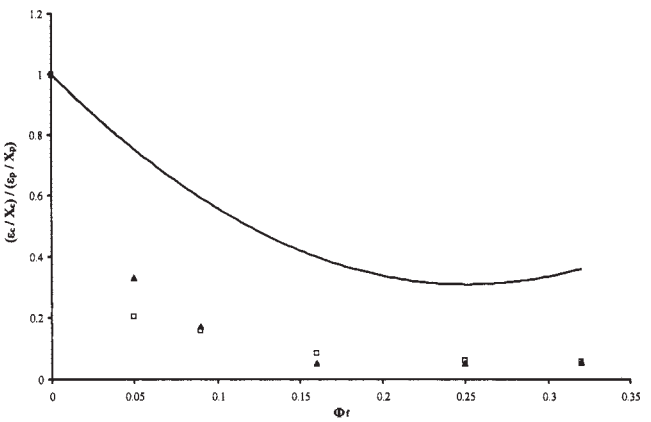

Figure 5 Comparison of normalized elongation-at-break of HDPE/TWF (□) and HDPE/TWF/HDPE-*g*-MAH (▲) composites with Nielsen's model with perfect adhesion, eq. (6), as a function of Φ_f.

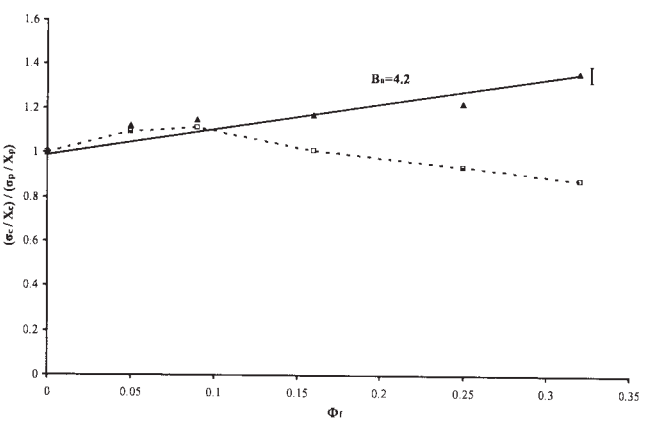

Figure 6 Comparison of normalized relative tensile strength with Bela Pukanszky model, eq. (7), with B_a value indicated in HDPE/TWF (□----) and HDPE/TWF/HDPE-*g*-MAH (▲——) composites vs. Φ_f.

TABLE I
Values of Reinforcement Parameter B_a, [eq. (6)], for HDPE/TWF and HDPE/TWF/HDPE-*g*-MAH Composites

	B_a	
Φ_f	(HDPE/TWF)	(HDPE/TWF/ HDPE-*g*-MAH)
0	–	–
0.05	5.1	5.7
0.09	4.5	4.8
0.16	3.3	4.2
0.25	2.8	3.9
0.32	2.7	4.0
Mean value		4.2

0.17 to 0.34. Because up to $\Phi_f = 0.09$ the tensile strength data were >1, the data were compared with Bela-Pukanszky model, Figure 6, [eq. (7)][37–42]:

$$(\sigma_c/X_c)/(\sigma_p/X_p) = (1 - \Phi_f/1 + 2.5\Phi_f)\exp(B_a\Phi_f) \quad (7)$$

Here, the term B_a describes the reinforcement and is denoted by "reinforcement factor." B_a values were estimated by comparing the normalized tensile strength data with [eq. (7)], Table I. The data up to $\Phi_f = 0.09$ agreed with the curve with $B_a = 4.2$, Curve I, whereas the values at $\Phi_f > 0.09$ deviated to a significant extent.

The increase of the tensile strength up to $\Phi_f = 0.09$ may be due to a reinforcing effect of the TWF. It was observed that in the presence of the TWF, the crystallinity of HDPE decreases, Figure 2, which should tend to decrease the tensile strength. However, the TWF also gives rise to mechanical restraint because of an anchoring effect arising out of differential thermal shrinkage.[31] The resultant of these two opposing effects will determine the composite behavior at the large deformation property, tensile breaking strength. As the effect of crystallinity has been eliminated, it could be argued that up to $\Phi_f = 0.09$ the effect of physical adhesion through the mechanical restraint takes dominance enhancing the tensile strength. At $\Phi_f > 0.09$ because of the absence of chemical adhesion, stress transfer is hindered and the physical adhesion becomes insufficient so that the tensile strength decreases. This is also aided by the filler agglomeration, where the composite is very weak because of weak bonding forces at the agglomerates.

In the presence of coupling agent, the normalized breaking strength data varied from 1 to 1.4 at $\Phi_f = 0$ to 0.34, Figure 6. This indicates the reinforcement of the HDPE by the TWF. The values of the reinforcement factor B_a are shown in Table I, and Curve I presents the plot of the model, [eq. (7)]. It can be seen that the data agree well with the model with an average $B_a = 4.2$, which implies a good extent of reinforcement of HDPE by the TWF. As the crystallinity decreased in the presence of the coupling agent, this increase in the tensile strength may be considered quite significant, similar to HDPE/BF composites.[6] The enhanced stress transfer or reinforcement may be attributed to increased chemical interaction of TWF with HDPE. The hydrocarbon moiety of the coupling agent, HDPE-*g*-MAH, is miscible with HDPE, whereas the anhydride moiety of maleic anhydride can chemically bind with hydroxyl groups of TWF (Scheme 1).[20,25]

Impact strength

Figure 7 presents the plot of normalized relative Izod impact strength, $(I_c/X_c)/(I_p/X_p)$, of HDPE/TWF composites against Φ_f. The impact strength decreases quite drastically to ~ 0.4 at $\Phi_f = 0.16$, the parameter then almost levels off at $\Phi_f > 0.16$. The decrease in the Izod impact property may be attributed to the decrease in deformability or increase in the stiffness of HDPE in the presence of TWF, similar to other such systems.[33] The stress concentration points formed around the TWF particles lead to crack initiation and failure at the impact mode of load application. The failure is more apparent because of a weak interphase in the absence of any strong phase interaction.

In the HDPE/TWF/HDPE-*g*-MAH composites, the impact strength also decreased in a similar manner, Figure 7. It was observed that the interphase interaction was to a degree stronger which enhanced tensile strength. However, it appears that as the coupling agent enhances the interactions to a limited extent (only 5% coupling agent was used based on TWF), it cannot eliminate the formation of stress concentration points. Thus, any residual discontinuity in the interphase would lead to

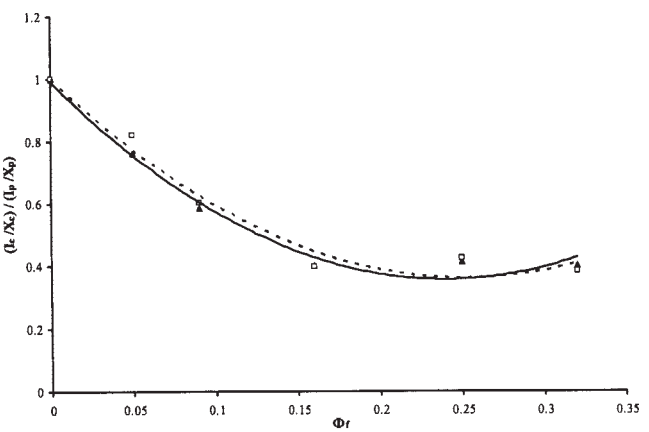

Figure 7 Plot of normalized relative Izod impact strength of HDPE/TWF (□----) and HDPE/TWF/HDPE-*g*-MAH (▲——) composites, against Φ_f.

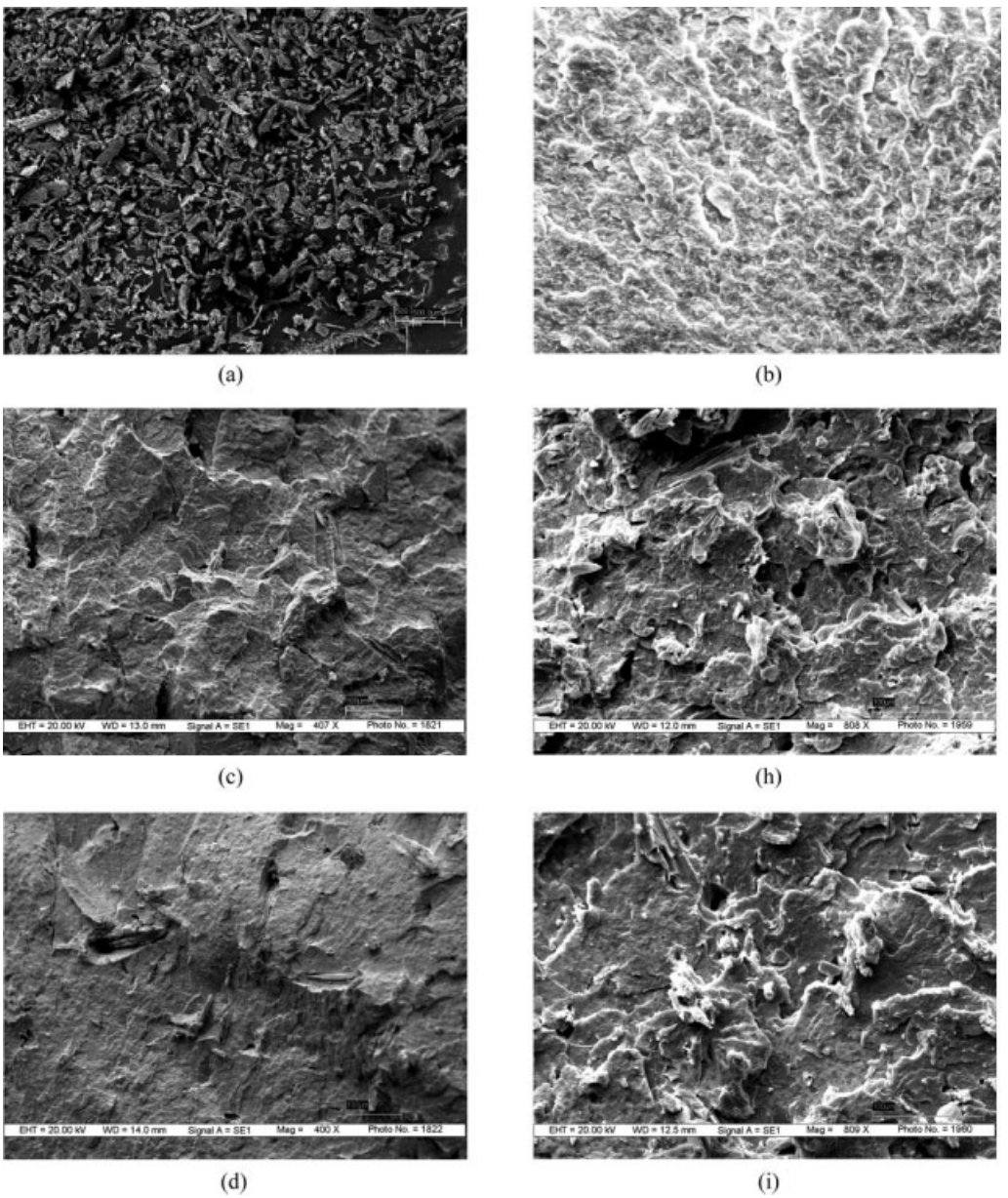

Figure 8 SEM micrographs of (a) teak wood flour, (b) HDPE and HDPE/TWF composites with varying Φ_f values: (c) 0.05, (d) 0.09, (e) 0.16, (f) 0.25, (g) 0.32. Micrographs of HDPE/TWF/HDPE-*g*-MAH composites at corresponding Φ_f values are presented in (h), (i), (j), (k), and (l).

catastrophic failure in the impact mode of stress application.

Fracture surface morphology

The SEM micrographs of HDPE, TWF, HDPE/TWF, and the HDPE/TWF/HDPE-*g*-MAH composites are shown in Figure 8(a–l). The TWF particles have uneven surfaces and vary in size, shape, and structure; some of the particles are longer in one dimension, Figure 8(a). The cryogenically fractured HDPE shows an undulated surface with a significant extent of whitening, Figure 8(b), which may arise because of tearing of the matrix, which in turn gives quite high impact strength, Figure 7. Upon addition of TWF, the fracture surface becomes concoidal, which indicates brittle type of composite structure, Figure 8(c–e), leading to decrease in impact strength, Figure 7. At still higher levels of TWF, the concoidal surfaces are seen strewn with filler particles with no polymer cover. The rough surface and the fiber pull out from the matrix during the breaking of samples indicate weak interfacial adhesion between the discrete and the matrix phase.

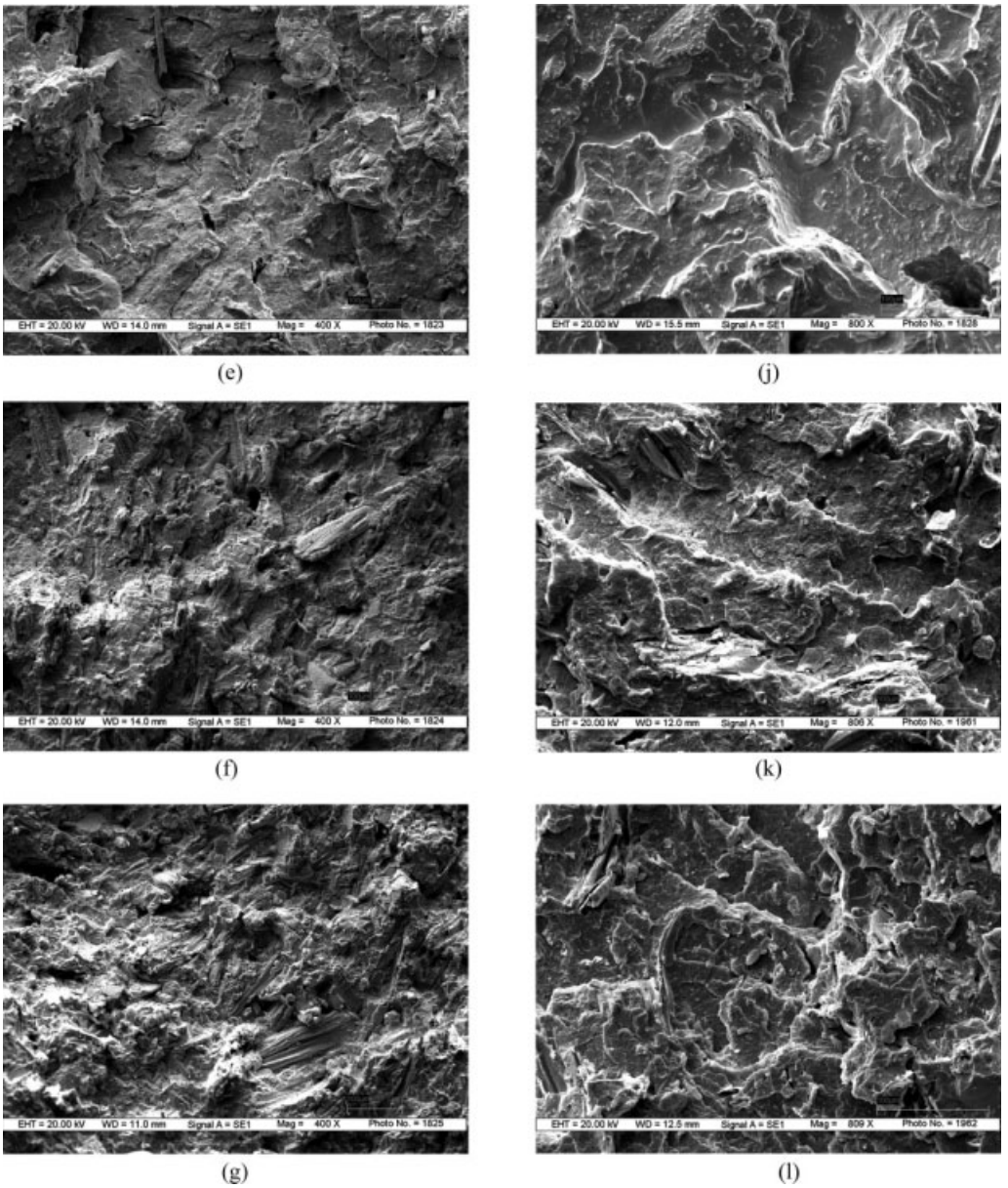

Figure 8 (*Continued from the previous page*)

In the presence of the coupling agent, the fracture surfaces were relatively smoother with adherent polymer residues on the TWF particles and some extent of stress whitening are seen, which arise because of enhanced phase interaction which stretches the polymer during fracture, Figure 8(h–l). HDPE/TWF/HDPE-*g*-MAH enhances the wetting of TWF with HDPE resulting in a degree of increased phase adhesion. However, this enhanced adhesion does not contribute to the improvement of impact strength because of poor stress transfer to the dispersed phase, as only a limited extent of surface adhesion occurred at a fixed concentration (5 wt % based on TWF content) of the coupling agent.

CONCLUSIONS

The tensile and impact properties of HDPE were modified in the presence of TWF. The tensile modulus and strength enhanced initially up to $\Phi_f = 0.09$, whereas at $\Phi_f > 0.09$ the properties decreased. The filler introduced mechanical restraints, decreased deformability and crystallinity of HDPE. Up to $\Phi_f = 0.09$, the former effect predominates, which enhanced both tensile modulus and strength. However, the formation of stress concentration and decrease in the crystallinity predominates at $\Phi_f > 0.09$, which decrease the tensile modulus and strength. Generation of stress concentrations and

mechanical restraints decreases the ductility of the matrix, which results in the decrease of both elongation-at-break and Izod impact strength of the composites.

Use of the coupling agent, HDPE-*g*-MAH, gave rise to a degree of chemical type of interphase adhesion. In addition with the mechanical restraints, this phase adhesion overrides the effect of decreased crystallinity of HDPE to enhance both tensile modulus and strength in the entire range of Φ_f (0.05–0.32). The elongation-at-break and Izod impact strength, however, decreased with increase in Φ_f. The enhanced phase adhesion functions as impediment to the matrix mobility similar to the HDPE/TWF composites.

The unmodified TWF particles were nonadherent with HDPE. Surface of separation of the particles are easily observed in the SEM photomicrographs. In the HDPE/TWF/HDPE-*g*-MAH composites, the particle boundaries are to an extent not distinct and the fracture surfaces are relatively smoother implying increased phase interaction.

References

1. Youngquist, J.; Myers, G. E.; Ageney, U.; Luther, W. M. Forest 1992, 2, 1.
2. Bledzki, A. K.; Gassan, J.; Theis, S. Mech Compos Mater 1998, 34, 563.
3. Forest Product Laboratory, Wood-Plastic Composites, Tech-Line; 2002, COM-1 01/04.
4. Bledzki, A. K.; Gassan, J. Prog Polym Sci 1999, 24, 221.
5. Yang, H.-S.; Wolcott, M. P.; Kim, H.-S.; Kim, S.; Kim, H.-J. Compos Struct 2007, 79, 369.
6. Sewda, K.; Maiti, S. N. J Appl Polym Sci 2007, 105, 2598.
7. Son, J.; Yang, H.-S.; Kim, H.-J. J Thermoplast Compos Mater 2004, 17, 509.
8. Matuana, L. M.; Balatinecz, J. J.; Sodhi, R. N. S.; Park, C. B. Wood Sci Technol 2001, 35, 191.
9. Jain, S.; Kumar, R.; Jindal, U. C. J Mater Sci 1992, 27, 4598.
10. Li, Q.; Matuana, L. M. J Thermoplast Compos Mater 2003, 16, 551.
11. Selke, S. E.; Wichman, I. Compos A 2004, 35, 321.
12. Joshi, S. V.; Drzal, L. T.; Mohanty, A. K.; Arora, S. Compos A 2004, 35, 371.
13. Maiti, S. N.; Hassan, M. R. J Appl Polym Sci 1989, 37, 2019.
14. Maiti, S. N.; Subbarao, R.; Ibrahim, M. N. J Appl Polym Sci 2004, 91, 644.
15. Maiti, S. N.; Singh, K. J Appl Polym Sci 1986, 32, 4285.
16. Brydson, J. A. Plastics Materials; Butterworth Heinemann: New York, 1999.
17. Stark, N. M.; Matuana, L. M.; Clemons, C. M. J Appl Polym Sci 2004, 93, 1021.
18. Riew, C. K.; Kinloch, A. J. Toughened Plastics I: Science and Engineering; American Chemical Society: Washington, DC, 1993.
19. Patil, Y. P.; Gajre, B.; Dusane, D.; Chavan, S.; Mishra, S. J Appl Polym Sci 2000, 77, 2963.
20. Yang, H. S.; Kim, H. J.; Park, H. J.; Lee, B. J.; Hwang, T. S. Compos Struct 2006, 72, 429.
21. Najafi, S. K.; Kiaefar, A.; Hamidina, E.; Tajvidi, M. J Reinf Plast Compos 2007, 26, 341.
22. Najafi, S. K.; Chaharmahli, M.; Tajvidi, M. J Appl Polym Sci 2006, 102, 3907.
23. Product Literature, GAIL. Available at: http://www.gailonline.com/petrochemicals/i58a180.htm.
24. Pluss Polymers, New Delhi, India. Available at: www.plusspolymers.com.
25. Stark, N. M.; Matuana, L. M. Polym Degrad Stab 2004, 86, 1.
26. ASTM. Annual Book of ASTM Standard, Part 37; ASTM: Philadelphia, 1976.
27. Khonakdar, H. A.; Jafari, S. H.; Taheri, M.; Wagenknecht, U.; Jehnichen, D.; Haüssler, L. J Appl Polym Sci 2006, 100, 3264.
28. Brandrup, J.; Immergut, E. H. Polymer Handbook; Wiley: New York, 1995.
29. Rusu, M.; Sofian, N.; Rusu, D. Polym Test 2001, 20, 409.
30. Ahmed, S.; Jones, F. R. J Mater Sci 1990, 25, 4933.
31. Nielsen, L. E. Mechanical Properties of Polymers and Composites; Marcel Dekker: New York, 1974.
32. Dolakova-Svehlova, V. J Macromol Sci Phys B 1982, 21, 231.
33. Maiti, S. N.; Mahapatro, P. K. J Appl Polym Sci 1991, 42, 3101.
34. Manson, J. A.; Sperling, L. H. Polymer Blends and Composites; Plenum: New York, 1976.
35. Colom, X.; Carrasco, F.; Pages, P.; Caňavate, J. Compos Sci Technol 2003, 63, 161.
36. Lu, J. Z.; Negulescu, I. I.; Wu, Q. Compos Interface 2005, 12, 125.
37. Pukanszky, B.; Belina, K.; Rockenbauer, A.; Maurer, F. H. J. Composites 1994, 25, 205.
38. Pukanszky, B.; Fekete, E.; Tüdös, F. Makromol Chem Macromol Symp 1989, 28, 165.
39. Danyadi, L.; Janecska, T.; Szabo, Z.; Nagy, G.; Moczo, J.; Pukanszky, B. Compos Sci Technol 2007, 67, 2838.
40. Liang, J. Z.; Li, R. K. Y. J Mater Process Technol 1998, 83, 127.
41. Nielsen, L. E. Mechanical Properties of Polymers and Composites; Marcel Dekker: New York, 1974; Vol. 2.
42. Maiti, S. N.; Mahapatro, P. K. Polym Compos 1990, 11, 223.